The Astrophysical Journal Supplement Series, 204:1 (8pp), 2013 January doi:10.1088/0067-0049/204/1/1

THE SPECTRUM OF Fe II

Gillian Nave[1] and Sveneric Johansson[2]
[1] National Institute of Standards and Technology, Gaithersburg, MD 20899-8422, USA; gillian.nave@nist.gov
[2] Lund Observatory, University of Lund, Box 43, SE-22100 Lund, Sweden
Received 2012 August 31; accepted 2012 October 16; published 2012 December 7

ABSTRACT

The spectrum of singly ionized iron (Fe II) has been recorded using high-resolution Fourier transform (FT) and grating spectroscopy over the wavelength range 900 Å to 5.5 μm. The spectra were observed in high-current continuous and pulsed hollow cathode discharges using FT spectrometers at the Kitt Peak National Observatory, Tucson, AZ and Imperial College, London and with the 10.7 m Normal Incidence Spectrograph at the National Institute of Standards and Technology. Roughly 12,900 lines were classified using 1027 energy levels of Fe II that were optimized to measured wavenumbers. The wavenumber uncertainties of lines in the FT spectra range from 10^{-4} cm^{-1} for strong lines around 4 μm to 0.05 cm^{-1} for weaker lines around 1500 Å. The wavelength uncertainty of lines in the grating spectra is 0.005 Å. The ionization energy of (130,655.4 ± 0.4) cm^{-1} was estimated from the 3d^6(^{5}D)5g and 3d^6(^{5}D)6h levels.

Key words: atomic data – line: identification – methods: laboratory

Online-only material: color figure, machine-readable tables

1. PREFACE

The title of Sveneric Johansson's last paper, "A Half-life of Fe II" (Johansson 2009), accurately describes his association with the spectrum during his career. He began work on the spectrum as a graduate student of Edlén, with papers on new energy levels (Johansson & Litzén 1974) and a comprehensive analysis of the spectrum (Johansson 1978). Much of his subsequent work focused on the discovery of new energy levels, identification of Fe II lines in astrophysical spectra, and their use for diagnostics, including the discovery of stimulated emission from Fe II in η Carinae (Johansson & Letokhov 2004). This work continued for the rest of his life, with his final paper on new energy levels in Fe II observable solely in stellar spectra (Johansson 2009), completed just days before his death in 2008.

In 1987, I began working on the spectrum of Fe I at Imperial College, London, UK (IC), using Fourier transform (FT) spectra of iron–neon and iron–argon hollow cathode lamps recorded at Kitt Peak National Observatory (KPNO) and IC. This work resulted in two papers on precise wavelengths in Fe I and Fe II (Nave et al. 1991, 1992). In 1992, I went to Lund University and began work with Sveneric to combine the FT spectra from IC with grating spectra recorded by him in 1988 on the 10.7 m normal incidence spectrograph at the National Institute of Standards and Technology (NIST). The combined data were used to produce a line list of about 34,000 spectral lines covering wavelengths from 833 Å to 5 μm. Roughly 9500 of these lines are due to Fe I, and these were used to produce optimized energy levels and a new Fe I multiplet table (Nave et al. 1994). About 15,000 of the remaining lines belong to Fe II. After completion of the work on Fe I, I continued to collaborate with Sveneric on the spectrum of Fe II, with the aim of preparing a comprehensive analysis and line list for Fe II. However, progress was slow due to competing work and his subsequent illness. Consequently, this work remained uncompleted when Sveneric died in 2008 October.

This paper is my best attempt to complete the analysis of Fe II in the way that Sveneric was unable to do. It has benefited from unpublished line lists and energy levels that he gave me while I was working in Lund and from the insights into the spectra of iron-group elements that I gained while there. However, the loss of Sveneric's knowledge and lack of access to some of the original data behind the unpublished line lists have resulted in some inconsistencies in the analysis. In particular, it has proven to be impossible to put the intensities on a consistent scale over the whole wavelength region. Since I do not have the original data behind the unpublished line lists, I was also unable to verify all of the lines in these lists in a way that I would have done otherwise. However, these lists appear to be reliable, and I have no reason to doubt that Sveneric prepared them well. Although Sveneric's considerable contributions of lines and energy levels make him a co-author of this paper, the final selection of lines and energy levels in the tables is solely mine.

Gillian Nave.

2. INTRODUCTION

The iron-group elements have complex spectra with thousands of lines from the VUV to the infrared (Johansson 1978). They are important in the absorption spectra of many astrophysical objects including the interstellar medium, hot and cool stars, gaseous nebulae, galaxies, and quasi-stellar object absorption line systems. Lines from Fe II in particular account for as many as half of the absorption features in A- and late B-type stars in all wavelength regions (Brandt et al. 1999). They also form prominent emission lines from a wide variety of objects including chromospheres of cool stars (Dupree et al. 2005), active galactic nuclei (Hamann & Ferland 1999), and nebular regions around massive stars.

Problems in modeling stellar spectra in the UV and VUV often can be traced to the lack of adequate data for iron-group elements, particularly for very highly excited levels of these elements. The importance of these highly excited levels has been demonstrated in observations of the Bp star HR6000 made with the HIRES spectrograph on the Very Large Telescope. Castelli et al. (2009) found it possible to identify strong lines in the region around 5178 Å as transitions of the 3d^6(^3H) 4d–4f array due to unpublished energy levels of Fe II. The upper levels

Table 1
Previous Work on Fe II

Reference	No. Energy Levels	No. Lines	Principal Configurations
Johansson (1978)	576	3272	$3d^6ns$, $3d^6np$, $3d^6nd$, $3d^64f$ $3d^5\ 4sns$,$(3d^54s)np$, $(3d^54s)4d$, $3d^54p^2$
Adam et al. (1987)	20	120	$3d^5\ 4s(^7S)4d$, $3d^5(^6S)4p^2$
Johansson & Baschek (1988)	73	...	$3d^6(^3L)4d$, where L = P, F, G, H
Nave et al. (1991)	...	221	
Rosberg & Johansson (1992)	49	220	$3d^6(^5D)5g$
Nave et al. (1997a)	...	473	
Biémont et al. (1997)	50	74	$3d^6(^5D)6h$
Castelli & Kurucz (2010)	109 (58 used)	137[a]	$3d^6(^3L)4f$,$3d^6(^3L)$nd where L = P, F, G, H
This work	102	12 909	

Notes. [a] Lines listed as laboratory measurements that are not included in Johansson (1978). 51 of the energy levels in Castelli & Kurucz (2010) could not be confirmed using our spectra.

of this transition array are located around 128,000 cm^{-1} (15 eV) and are the highest known levels of Fe II.

Previous papers on Fe II containing substantial numbers of lines or energy levels are summarized in Table 1. The last comprehensive publication on Fe II was in 1978 (Johansson 1978). It contained classification of 3272 lines from 576 energy levels, covering the wavelength range 900 Å to 11 200 Å. The wavelength uncertainty of the best lines was 0.02 Å. Since then, precise wavelengths of Fe II in the UV (Nave et al. 1991; Nave & Sansonetti 2004) and VUV (Nave et al. 1997a) have been published. Additional Fe II wavelengths have been reported by Adam et al. (1987), Rosberg & Johansson (1992), Johansson et al. (1995), Biémont et al. (1997), Aldenius et al. (2006), Aldenius (2009), Castelli et al. (2009), and Castelli & Kurucz (2010). These publications contain approximately 500 new spectral lines. Studies by Adam et al. (1987), Johansson & Baschek (1988), Rosberg & Johansson (1992), Biémont et al. (1997), and Castelli & Kurucz (2010) account for an additional 301 new energy levels.

3. EXPERIMENTAL WORK

The laboratory spectra used here are the same as those in our previous studies of Fe I and Fe II (Nave et al. 1991, 1992, 1994, 1997a). The spectra were obtained on four different instruments: the $f/55$ IR–visible–UV Fourier transform (FT) spectrometer at the Kitt Peak National Observatory (KPNO), Tucson, AZ for the region 2000 cm^{-1} to 35 000 cm^{-1} (5 μm to 2900 Å); the $f/25$ vacuum UV FT spectrometer at Imperial College, London (IC) for the region 33,000 cm^{-1} to 67,000 cm^{-1} (3000 Å to 1500 Å); the $f/25$ UV FT spectrometer at Lund University, Sweden for the region 31,900 cm^{-1} to 55,000 cm^{-1} (3135 Å to 1820 Å); and the 10.7 m Normal Incidence Grating Spectrograph at NIST for high-dispersion grating spectra above 30 770 cm^{-1} (<3250 Å).

3.1. Fourier Transform Spectra

The light source used for the FT investigations was a hollow cathode lamp, run in either neon or argon. This source emits lines of Fe I, Fe II, the neutral and singly ionized spectra of the carrier gas used, and a small number of impurities. The cathode was a 35 mm long cylinder of pure iron with an 8 mm bore. A water cooled cathode was used for some of the spectrograms. The metal case of the lamp formed the anode. The gas pressures were about 500 Pa of Ne or 400 Pa of Ar for the visible and IR observations made at KPNO, and 300 Pa to 800 Pa of Ne for the UV observations made at IC. The currents ranged from 320 mA to 1.1 A. Argon–iron spectra were recorded in the region 17,500 cm^{-1} to 35,000 cm^{-1} to provide an absolute wavelength calibration based on Ar II lines. One infrared spectrum was recorded with a water-cooled cathode as source and a higher current of 1.4 A. The spectra are summarized in Table 2.

The wavenumber, integrated intensity, and width of all lines in the FT spectra were obtained using the Decomp program of Brault & Abrams (1989) and its modification Xgremlin (Nave et al. 1997b), which fit Voigt profiles to the spectral lines. Each line was measured in up to nine different spectra. The FWHM of the lines varied from about 0.024 cm^{-1} at 5000 cm^{-1} (0.1 Å at 2 μm) to about 0.24 cm^{-1} at 50,000 cm^{-1} (10 mÅ at 2000 Å).

The spectra were calibrated with lines of Ar II between 19,429 cm^{-1} and 22,826 cm^{-1} taken from Whaling et al. (1995). The calibration was carried into the UV and infra-red using wide-range spectra (Nave et al. 1991, 1992). Details of the calibration of the visible and UV spectra are given in Nave & Sansonetti (2011), and of the IR spectra in Nave et al. (1992). The calibration of the UV spectra based on Ar II agrees to better than 1:10^8 with a calibration based on Mg I and Mg II lines measured with a frequency comb (Salumbides et al. 2006; Hannemann et al. 2006; Batteiger et al. 2009).

The uncertainty of the wavenumber of a line measured in a single spectrum is a sum in quadrature of the statistical uncertainty in the measurement of its position and of the calibration uncertainty for the whole spectrum. The statistical uncertainty was estimated from the FWHM of the line divided by twice the signal-to-noise ratio (S/N). This was derived from Equation (9.3) of Davis et al. (2001), assuming four statistically independent points in a line width. The S/N was estimated using a global noise level for each spectrum, but was limited to 100 for strong lines for the purposes of calculating the uncertainty. This accounts for an increased noise level around the strongest lines in the KPNO spectra due to low frequency ghosts and also ensures that strong lines measured in more than one spectrum receive similar weighting in the calculation of uncertainty of the weighted mean wavenumber. The statistical uncertainty of strong lines (S/N > 100) varies from 0.0001 cm^{-1} (0.8 mÅ at 2 μm) in the infrared to 0.001 cm^{-1} (0.01 mÅ at 3000 Å) in the ultraviolet. The weakest lines in the spectra have an S/N of about 3, and their uncertainty varies from about 0.005 cm^{-1} (0.02 Å at 2 μm) in the infrared to 0.05 cm^{-1} (5 mÅ at 3000 Å) in the ultraviolet. For lines measured in several spectra, a weighted average wavenumber and uncertainty were calculated using the squared reciprocal of the statistical uncertainty as a

Table 2
Spectra Used in this Analysis[a]

Name[b]	Lower Wavenumber (cm^{-1})	Upper Wavenumber (cm^{-1})	Resolution (cm^{-1})	Gas	Pressure Pa (Torr)	Current A	Notes
KPNO FT Spectrometer CaF_2 beamsplitter							
820216R0.001	2006	8996	0.012	Ne	373 (2.8)	1.4	Water cooled cathode; N6 in Nave et al. (1992)
801211R0.002	5007	5544	0.0095	Ne	533 (4.0)	0.85	N1 in Nave et al. (1992)
KPNO FT spectrometer. Visible–UV beamsplitter							
800321R0.001	5000	9436	0.012	Ne	533 (4.0)	0.86	N2 in Nave et al. (1992)
810731R0.007	5007	11 743	0.015	Ne	546 (4.1)	1.04	
810731R0.009	10 343	13 350	0.020	Ne	560 (4.2)	1.05	N3 in Nave et al. (1992)
810731R0.005	10 505	13 820	0.018	Ne	546 (4.1)	1.04	
810622R0.021	18 024	35 984	0.043	Ne	533 (4.0)	0.75	k11 in Nave et al. (1991); N2 in Learner & Thorne (1988)
810622R0.009	17 198	34 040	0.043	Ar	400 (3.0)	0.4	k19 in Nave et al. (1991); A1 in Learner & Thorne (1988)
810724R0.003	16 013	17 950	0.025	Ar	413 (3.1)	1.0	
810724R0.002	20 801	26 000	0.036	Ar	400 (3.0)	1.0	
800325R0.007	14 220	17 060	0.025	Ar	400 (3.0)	0.81	
810622R0.012	17 006	25 000	0.033	Ne	533 (4.0)	0.75	N1 in Learner & Thorne (1988)
IC FT spectrometer							
fe6	33 000	44 500	0.07	Ne	533 (4.0)	0.75	
i74	35 000	46 000	0.105	Ne	400 (3.0)	0.35	
i20	41 500	48 000	0.17	Ne	333 (2.5)	0.95	
i22	41 500	48 000	0.17	Ne	333 (2.5)	0.95	
i24	38 000	44 000	0.17	Ne	333 (2.5)	0.95	
fen180	44 000	59 000	0.08	Ne	800 (6.0)	0.5	
fen200	44 000	59 000	0.08	Ne	800 (6.0)	0.5	
fe7	56 000	75 000	0.07	Ne	[c]	0.5	
fe8	50 300	67 000	0.08	Ne	[c]	0.5	
Lund FT spectrometer							
fe04193	31 600	47 000	0.07	Ar/Ne	[c]	1.0	
fe04201	31 600	47 000	0.07	Ne	67 (0.5)	1.0	

NIST Normal Incidence Grating Spectrograph

	Lower Wavelength (Å)	Upper Wavelength (Å)	Gas	Pressure Pa (Torr)	Current A	Notes
plate 8,6°	836	1523	Ne	130 (1.0)	0.66	Pulsed, 100 A peak, pulse width 70 μs, 100 Hz
plate 8,6°	836	1523	Ar	40 (0.3)	0.61	Pulsed, 100 A peak, pulse width 70 μs, 100 Hz
plate 4,8°	1400	2107	Ne	130 (1.0)	0.64	Pulsed, 100 A peak, pulse width 60 μs, 100 Hz
plate 4,8°	1400	2107	Ar	40 (0.3)	0.64	Pulsed, 100 A peak, pulse width 60 μs, 100 Hz

Notes.
[a] Additional grating spectra were taken between 2107 Å and 3249 Å under conditions similar to the above spectra. Line lists for these spectra were given to G. Nave by S. Johansson in the early 1990s but full details are not known. Roughly 2000 Fe II lines have been taken from these spectra and are included in Table 4.
[b] Name of spectrum in the National Solar Observatory digital Library (Hill & Suarez 2012).
[c] The pressure was not recorded for these archival spectra.

weight. Since the statistical uncertainties of the individual lines are uncorrelated, their squared reciprocal was also used as a weighting factor in the optimization of the energy levels.

The calibration uncertainty of a spectrum consists of two parts: the uncertainty of the original standards and the uncertainty of the calibration constant derived from those standards. The uncertainty of the original Ar II standards is 2×10^{-4} cm^{-1}. These Ar II standards are used to calibrate a "master spectrum," covering the wavenumber region 17,200 cm^{-1} to 34,040 cm^{-1} (810622R0.009 in Table 2), with a one standard uncertainty of 1.8 parts in 10^8. This calibration is propagated to the UV and IR regions using overlapping spectra, each of which increases the calibration uncertainty. The shortest UV spectrum (fe7 in Table 2) thus has the largest calibration uncertainty of 4 parts in 10^8. The calibration uncertainty for a particular line can thus vary, depending on how the spectra in which it was measured were calibrated. For simplicity, we adopted a global calibration uncertainty of four parts in 10^8 for all spectral lines. Since this calibration uncertainty is common to all lines, it is not included in the optimization of the energy levels, but is added in

quadrature to the uncertainties of the optimized energy level values after the optimization.

3.2. Grating Spectra

Grating spectra were recorded in the region 30,770 cm^{-1} to 119,617 cm^{-1} (3250 Å to 836 Å) using iron–neon and iron–argon hollow cathode lamps. The iron–neon hollow cathode lamp was run in pulsed mode with a peak current of 100 A, pulse width of 70 μs, pulse frequency of 100 Hz, and a gas pressure of 130 Pa. The iron–argon hollow cathode lamp was run in pulsed mode under similar conditions with a gas pressure of about 40 Pa. Similar spectra were recorded with a continuous hollow cathode lamp for comparison, but the results are not presented here. Details of the grating spectra are given in Table 2.

Spectra of the pulsed iron–neon hollow cathode between 850 Å and 2107 Å were read from the photographic plates using an automatic comparator at Lund University that produced a signal proportional to the optical density of the plate integrated over the full height of the slit image. This produced a file of optical density of the recorded spectrum as a function of position along the direction of dispersion. This file was read in to Xgremlin and Gaussian profiles were fitted to the spectral lines to obtain the wavelength and peak intensity. Strong spectral lines saturate the image on the photographic plates and give profiles with a flat top that cannot be fitted with a Gaussian profile. The centroid of these lines was estimated by integrating the profile between two points taken on either side of the line profile. These wavelengths are, however, less reliable than those obtained by fitting the line profile with a Gaussian.

Additional lines in the spectra listed in Table 2 are present in line lists given to G. Nave by S. Johansson in 1992. These are all either weak lines that are visible on the photographic plates but not easily fit by the Xgremlin software or lines blended with much stronger lines. Roughly 360 lines of this type between 850 Å and 1600 Å have been included in Table 4. Line lists for additional spectra between 1600 Å and 3250 Å were given to G. Nave by S. Johansson in the mid-1990s. These were obtained from spectra recorded under similar conditions to the spectra in Table 2, but full details of those spectra are not known. Roughly 2200 lines from these spectra are included in Table 4.

All grating spectra were calibrated from Ritz wavelengths of Fe II lines derived from energy levels determined from the FT spectra, with particular care being taken to avoid lines that were weak, were saturated on the photographic plate, or were significantly asymmetric. The wavelength uncertainty of these calibration lines is approximately 2 mÅ. Details of the calibration procedure are given in Nave et al. (1997a).

4. LINE IDENTIFICATIONS

The initial identification of the lines was performed solely in the FT spectra. These line identifications were carefully examined to eliminate spurious coincidences of lines and energy level differences and were then used to obtain optimized values for many of the energy levels. The remaining levels were found using unidentified lines in the FT and grating spectra and the identifications were again examined to eliminate spurious coincidences. Finally, both the FT and grating spectra were used to obtain optimized energy level values and Ritz wavelengths and wavenumbers. The full procedure is as follows.

About 28,000 lines were measured in the FT spectra. Known lines that belong to species other than Fe II were identified by comparison to previously published wavelengths in Fe I (Nave et al. 1994), Ar I–II (Whaling et al. 1995, 2002), Ne I–III (Sansonetti et al. 2004; Saloman & Sansonetti 2004; Kramida & Nave 2006), and various impurities present in the spectra (Ralchenko et al. 2012). An initial identification of Fe II lines was made by comparison with Ritz wavelengths calculated from Fe II energy levels taken from the references in Table 1. Many of these levels had large uncertainties as they were obtained from grating spectra of lower resolution and accuracy than our FT spectra. Setting a large tolerance window for the agreement between the Ritz and experimental wavelengths leads to many spurious identifications of lines from these levels. A better approach is to use a few lines known to combine with these levels to obtain a better value for the energy level. The energy levels then have low uncertainties and the tolerance window can be set lower, leading to fewer spurious identifications.

Roughly 10,000 lines in the FT spectra matched energy level differences in Fe II. About 1/3 of these lines had more than one possible identification. The identifications of all lines were checked to ensure that very few spurious identifications contributed to the energy level optimization, as even a small number of misidentified lines can have a significant effect on the optimized energy levels. This task was aided by the small uncertainty of the wavenumbers obtained from an FT spectrometer, and by predicted intensities from the atomic structure calculations of Kurucz (2010). Although the accuracy of these calculations is limited by strong configuration interaction in Fe II, they were useful for locating lines in FT spectra from levels that had been found using less accurate data from grating spectrographs. After eliminating spurious identifications, the total number of Fe II lines in the FT spectra was 8930, of which 798 had more than one plausible identification.

The lines measured in FT spectra were used to derive optimized energy levels and Ritz wavenumbers using the computer program lopt (Kramida 2011). Values for 942 energy levels of Fe II were derived from 8930 lines covering wavenumbers from 2008 cm^{-1} to 67,851 cm^{-1}. The line uncertainties assigned for use in the level optimization omit the calibration uncertainty (see Section 3.1). The statistical uncertainty, estimated as described in Section 3.1, was added in quadrature to a minimum estimated uncertainty of 0.001 cm^{-1}. This value was chosen to ensure that the level optimization was not dominated by the infrared region, where narrow linewidths give very precise wavenumbers, but the calibration uncertainty of the spectra is higher as many overlapping spectra are required to reach the Ar II standards. Weights were then assigned proportional to the squared reciprocal of the estimated uncertainty of the wavenumber of the line. Lines with more than one possible classification, lines that were blended, and lines with a large difference between the observed and Ritz wavenumber were assigned a low weight so that they did not significantly affect the values of the optimized energy levels.

The optimization was performed in three different steps. The first step was designed to obtain accurate values and uncertainties for the ground term, a^6D. The values for the a^6D intervals can be determined from differences between lines close to one another in the same spectrum sharing the same calibration, hence the calibration uncertainty does not contribute to the uncertainty in the relative values of these energy levels. An optimization was thus performed with a set of lines connecting the lowest a^6D term to higher $3d^6\,(^5D)4p$ levels. These lines were assigned a weight proportional to the squared reciprocal of the statistical uncertainty of the wavenumber. The minimum estimated uncertainty of 0.001 cm^{-1} was omitted as all the lines

Table 3
Energy Levels of Fe II

Assigned Configuration	Term	J	Level (cm^{-1})	Uncertainty[a] (cm^{-1})	No. of Lines
$3d^6(^5D)4s$	a^6D	9/2	0.0000	0.0000	42
		7/2	384.7872	0.0003	60
		5/2	667.6829	0.0003	64
		3/2	862.6118	0.0004	52
		1/2	977.0498	0.0004	30
$3d^7$	a^4F	9/2	1872.5998	0.0006	63
		7/2	2430.1369	0.0006	77
		5/2	2837.9807	0.0007	76
		3/2	3117.4877	0.0008	54
$3d^6(^5D)4s$	a^4D	7/2	7955.3186	0.0007	65
		5/2	8391.9554	0.0007	72
		3/2	8680.4706	0.0007	58
		1/2	8846.7837	0.0008	32
$3d^7$	a^4P	5/2	13474.4474	0.0009	67
		3/2	13673.2045	0.0010	63
		1/2	13904.8604	0.0012	38
	a^2G	9/2	15844.6485	0.0012	55
		7/2	16369.4098	0.0013	59
	a^2P	3/2	18360.6399	0.0016	42
		1/2	18886.773	0.002	29
	a^2H	11/2	20340.2461	0.0013	43
		9/2	20805.7632	0.0014	57
	a^2D2	5/2	20516.9534	0.0016	62
		3/2	21307.999	0.002	47
$3d^6(^3P2)4s$	b^4P	5/2	20830.5534	0.0011	75
		3/2	21812.0454	0.0012	61
		1/2	22409.8178	0.0013	47

Note. [a] One standard uncertainty.

(This table is available in its entirety in a machine-readable form in the online journal. A portion is shown here for guidance regarding its form and content.)

are in the same spectral region. In the second step, the a^6D levels were fixed to the values and uncertainties determined from the first step. The weights of all the lines in the FT spectra were assigned by combining in quadrature the statistical uncertainty and the minimum estimated uncertainty of 0.001 cm^{-1} in order to obtain accurate uncertainties for the $3d^6(^5D)4p$ and higher levels.

After the second step of the level optimization, a further 86 energy levels that had not been optimized with the FT spectra were added. Most of these were from Biémont et al. (1997) and Castelli & Kurucz (2010). Roughly half of the levels in Castelli & Kurucz (2010) could not be matched definitively to lines in the FT spectra. Levels were adopted from Castelli & Kurucz (2010) if they had strong transitions that matched at least two lines in the FT spectra. All the energy levels were then used to identify additional lines in both the FT and grating spectra. The final optimization step derived values for 1027 energy levels from 13,653 transitions in both FT and grating spectra, again fixing the values of the a^6D levels to the values obtained in the first step. An uncertainty of 0.005 Å was assigned to all grating lines. The energy level uncertainties from this iteration were added in quadrature to a global calibration uncertainty of 4×10^{-8} times the value of the energy level.

5. ENERGY LEVELS AND LINES

The 1027 energy levels is given in Table 3. The configurations and terms in Columns 1 and 2 are taken from the NIST Atomic Spectra Database (Ralchenko et al. 2012), the papers in Table 1, or the calculations of Kurucz (2010). Many of the levels between 114,212 cm^{-1} and 114,673 cm^{-1} have not been assigned to configurations. The levels in this region are from the two overlapping configurations $3d^6(^5D)6d$ and $3d^6(^3D)4d$. The energy level values are given in Column 4. The uncertainties with respect to the ground term are given in Column 5 and represent one standard uncertainty. They were obtained from the LOPT program by combining the uncertainties derived from the level optimization in quadrature with a global calibration uncertainty of 4×10^{-8} times the level value. The last column lists the number of observed lines that combine with the level.

The table of observed Fe II lines (13,653 transitions) is given in Table 4. The intensities in Column 1 depend on the source conditions and method of measurement. The wavenumbers and intensities of all of the lines above 3250 Å were taken from a weighted average of up to nine individual measurements in the FT spectra. Since these intensities were measured using several different source conditions, they are useful only as a guide to the approximate strength of the line and should not be relied upon for accurate intensity measurements. Wavenumbers and intensities of lines below 3250 Å that are marked with an "F" in Column 11 were also taken from FT spectra. The wavelengths and intensities of lines marked "G" in Column 11 are from the grating spectra of the pulsed iron–neon hollow cathode lamp listed in Table 2. The intensity scale of the grating lines is different from the intensity scale of the FT spectra and is given as decimal numbers in Table 4. Strong lines that saturate the photographic plate are indicated with an "S" in Column 11. Wavelengths and intensities of lines taken from the additional line lists are indicated with "N" in Column 11 if taken from the pulsed iron–neon hollow cathode, "A" if taken from the pulsed iron–argon hollow cathode lamp. The intensities are visual estimates of the photographic density and are also given as decimal numbers, ranging from 0 to 5 for most lines. The intensity scale is different from both the lines in the FT spectra and the grating spectra lines marked with a "G." Lines marked "b" are broad, those marked "0d" are faint and diffuse and those marked "0d?" are hardly detectable from the background. Lines below 1600 Å taken from the line lists given to G. Nave by S. Johansson have uncertain intensities as they are all weak or blended. They have been assigned an intensity of "00" and indicated with "L" in Column 11.

The wavelength in Column 2 was derived from the wavenumber in Column 4 for lines taken from the FT spectra. Air wavelengths, given for lines between 2000 Å and 2 μm, were derived from the five parameter formulae in Equation (3) of Peck & Reeder (1972). The wavelengths were measured directly in the grating spectra and the wavenumbers derived from them. The corresponding one standard uncertainties in Columns 3 and 5 include contributions from the statistical uncertainty in the measurement of the position of the line and the calibration uncertainty for the spectrum. The one standard uncertainty of lines taken from grating spectra has been estimated at 0.005 Å. Ritz wavelengths and their statistical uncertainties were obtained from LOPT and are given in Columns 6 and 7, respectively. The uncertainties were derived by adding the uncertainties from LOPT to a global calibration uncertainty of 4×10^{-8}. The classification of the line is given in Column 10, with the values of the lower and upper energy levels in Columns 8 and 9, respectively. In addition to the codes indicating the source of the data, Column 11 also indicates if there are any other identifications for the line.

Table 4
Observed Lines of Fe II

Intensity[a]	Vacuum Wavelength (Å)	Uncertainty[b] (Å)	Wavenumber (cm^{-1})	Uncertainty[b] (cm^{-1})	Ritz Vacuum Wavelength (Å)	Uncertainty[b] (Å)	Lower Level (cm^{-1})	Upper Level (cm^{-1})	Classification				Notes[c]
0.9	1824.980	0.005	54 795.13	0.06	1824.979 49	0.000 11	20 805.7632	75 600.900	$3d^7$	$a^2H_{9/2}-$	$3d^6(^3D)4p$	$w^2F^\circ_{7/2}$	G
0	1824.860	0.005	54 798.73	0.15	1824.860 52	0.000 08	67 516.328	122 315.037	$3d^6(^3G)4p$	$y^2H^\circ_{11/2}-$	$3d^6(^3H)6s$	$^2H_{11/2}$	N
0	1823.929	0.005	54 826.70	0.15	1823.929 60	0.000 12	18 360.6399	73 187.318	$3d^7$	$a^2P_{3/2}-$	$3d^6(^3D)4p$	$y^2P^\circ_{1/2}$	N
4	1823.8711	0.0008	54 828.44	0.02	1823.869 85	0.000 10	18 360.6399	73 189.114	$3d^7$	$a^2P_{3/2}-$	$3d^6(^3D)4p$	$y^2P^\circ_{3/2}$	F
1.0	1822.196	0.005	54 878.83	0.06	1822.189 74	0.000 08	8 680.4706	63 559.498	$3d^6(^5D)4s$	$a^4D_{3/2}-$	$3d^6(^3F2)4p$	$x^4D^\circ_{1/2}$	G II
1.0	1822.196	0.005	54 878.83	0.06	1822.190 10	0.000 19	44 929.532	99 808.549	$3d^6(^1F)4s$	$c^2F_{5/2}-$	$3d^6(^1G1)4p$	$^2G^\circ_{7/2}$	G II
1.3	1822.135	0.005	54 880.67	0.15	1822.123 38	0.000 08	8 391.9554	63 272.981	$3d^6(^5D)4s$	$a^4D_{5/2}-$	$3d^6(^3F2)4p$	$x^4D^\circ_{5/2}$	S
4	1820.9161	0.0008	54 917.41	0.03	1820.916 18	0.000 08	54 232.201	109 149.611	$3d^5\,4s^2$	$b^4G_{11/2}-$	$3d^5(^2I)\,4s4p(^3P)$	$^2I^\circ_{13/2}$	F
0.9	1820.480	0.005	54 930.58	0.06	1820.478 44	0.000 17	31 999.049	86 929.664	$3d^7$	$b^2F_{7/2}-$	$3d^6(^3P1)4p$	$v^4D^\circ_{7/2}$	G
1.0	1819.643	0.005	54 955.82	0.06	1819.644 13	0.000 14	31 811.814	86 767.614	$3d^7$	$b^2F_{5/2}-$	$3d^6(^3P1)4p$	$v^4D^\circ_{5/2}$	G
9	1818.5202	0.0003	54 989.767	0.010	1818.521 51	0.000 08	7 955.3186	62 945.045	$3d^6(^5D)4s$	$a^4D_{7/2}-$	$3d^6(^3F2)4p$	$x^4D^\circ_{7/2}$	F *
0	1816.086	0.005	55 063.48	0.15	1816.085 38	0.000 08	46 967.4751	102 030.965	$3d^6(^5D)4p$	$z^4P^\circ_{5/2}-$	$3d^6(^5D)6s$	$^6D_{7/2}$	N
1.3	1815.766	0.005	55 073.17	0.15	1815.765 92	0.000 08	8 391.9554	63 465.134	$3d^6(^5D)4s$	$a^4D_{5/2}-$	$3d^6(^3F2)4p$	$x^4D^\circ_{3/2}$	S
4	1815.4116	0.0005	55 083.927	0.016	1815.410 97	0.000 11	20 516.9534	75 600.900	$3d^7$	$a^2D2_{5/2}-$	$3d^6(^3D)4p$	$w^2F^\circ_{7/2}$	F
0d?	1810.261	0.005	55 240.66	0.15	1810.262 75	0.000 11	54 904.241	110 144.841	$3d^6(^3F1)4s$	$d^2F_{7/2}-$	$3d^6(^3F)5p$	$^4F^\circ_{7/2}$	N
0	1810.117	0.005	55 245.06	0.15	1810.110 58	0.000 11	61 093.406	116 338.649	$3d^6(^3P2)4p$	$z^2D^\circ_{5/2}-$	$3d^5\,4s(^7S)4d$	$^6D_{5/2}$	N Ne
0d?	1809.945	0.005	55 250.31	0.15	1809.944 8	0.001 0	50 157.475	105 407.78	$3d^6(^3F1)4s$	$c^4F_{9/2}-$	$3d^5(^2D)\,4s4p(^3P)$	$^4F^\circ_{9/2}$	N
6	1809.3168	0.0008	55 269.48	0.02	1809.318 25	0.000 11	21 307.999	76 577.436	$3d^7$	$a^2D2_{3/2}-$	$3d^6(^1S2)4p$	$x^2P^\circ_{1/2}$	F
2.	1809.291	0.005	55 270.28	0.15	1809.288 12	0.000 08	42 237.0575	97 507.414	$3d^6(^5D)4p$	$z^6F^\circ_{7/2}-$	$3d^6(^3P2)5s$	$^4P_{5/2}$	N

Notes.

[a] Intensities of the lines with different codes in the "Notes" column are on different scales and should not be relied on for accurate intensity measurements. Decimal numbers are from grating spectra. Integer numbers are from FT spectra, which are in general the stronger lines. Intensities labeled "00" below 1600 Å are from unpublished line lists. Intensities labeled "d" are diffuse; those marked "d0?" are faint and diffuse; those marked "b" are broad.

[b] One standard uncertainty of preceding column.

[c] *: Line given low weight in level optimization; F: Line measured in FT spectra;
G: Line measured in grating spectra;
N: Line is from unpublished iron-neon line lists (see Section 3.2).
A: Line is from unpublished iron-argon line lists (see Section 3.2).
L: Line is from unpublished line lists below 1600 AA (see Section 3.2).
S: Line measured in grating spectra and is saturated on plate.
I, II, III : Line blended with Fe I, Fe II, or Fe III.
Ne, Ar, Si, Ti, Cr, Co, Ni : Line blended with species indicated.
gh : Line possibly blended with ghost.

(This table is available in its entirety in a machine-readable form in the online journal. A portion is shown here for guidance regarding its form and content.)

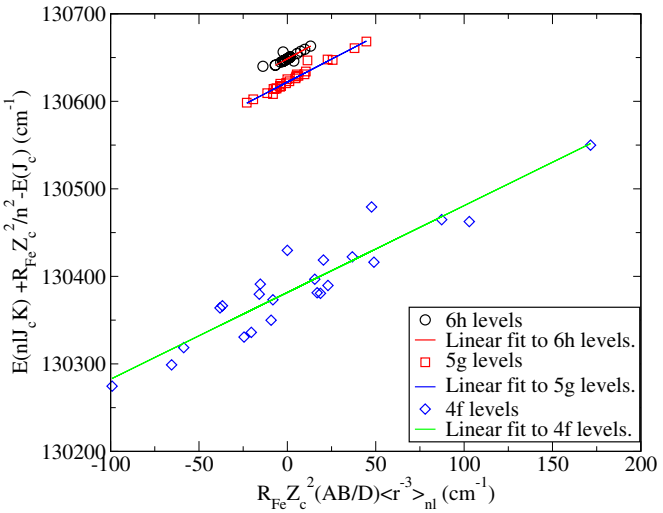

Figure 1. Calculation of the ionization energy for Fe II from the $3d^6(^5D)4f$, $3d^6(^5D)5g$, and $3d^6(^5D)6h$ levels. The intercept for each configuration is $IE - \alpha R_{Fe} Z_c^2 \langle r^{-4} \rangle_{nl}$.

(A color version of this figure is available in the online journal.)

6. IONIZATION ENERGY

Johansson (1978) obtained an estimate of 130 563 ± 10 cm^{-1} for the ionization energy of Fe II by using a two-parameter fit to the highest J-value levels of the lowest three $3d^6(^5D)ns$ configurations and comparing the value to similar terms in other singly ionized iron-group elements. A better estimate can be obtained by using highly excited levels that are well described by the J_cK coupling scheme.

We have used the quadrupole-polarization model of Schoenfeld et al. (1995) to obtain the ionization energy from the $3d^6(^5D)4f$, $3d^6(^5D)5g$, and $3d^6(^5D)6h$ levels. The outer electron in these levels is weakly bound to the core and the levels form five groups, separated by the fine structure intervals of the $3d^6\,{}^5D$ term of Fe III. Within each group the levels form pairs and the energy of the center of gravity of the pairs, $E(nlJ_cK)$, can be described by

$$E(nlJ_cK) = \mathrm{IE} + E(J_c) - R_{\mathrm{Fe}} Z_c^2 \Big(1/n^2 + \alpha \langle r^{-4} \rangle_{nl} - \frac{AB}{D} Q \langle r^{-3} \rangle_{nl} \Big), \quad (1)$$

where IE is the ionization energy, $E(J_c)$ is the energy of the $3d^6\,{}^5D_{J_c}$ level in Fe III, R_{Fe} is the Rydberg constant for Fe II (109 736.248 cm^{-1}), Z_c is the effective charge of the core (2 for Fe II), $\langle r^{-3} \rangle_{nl}$ and $\langle r^{-4} \rangle_{nl}$ are hydrogenic radial expectation values in atomic units given by Equations (3) and (4) of Schoenfeld et al. (1995), and A, B, and D are given by Equation (5) of Schoenfeld et al. (1995). The dipole polarizability α of the core and its quadrupole moment Q in atomic units are obtained from the experimental energy levels. By plotting $E(nlJ_cK) + R_{\mathrm{Fe}} Z_c^2/n^2 - E(J_c)$ for each configuration against $R_{\mathrm{Fe}} Z_c^2 (AB/D) \langle r^{-3} \rangle_{nl}$, a straight line of slope Q and intercept IE $- \alpha R_{Fe} Z_c^2 \langle r^{-4} \rangle_{nl}$ is obtained. This is shown in Figure 1. The ionization energy and α can then be obtained by simultaneously solving the equations for the intercepts for pairs of configurations.

The values of Q obtained from the slopes in Figure 1 are 0.99 ± 0.08 ea_o^2 (where e is the elementary charge and a_o the Bohr radius) for the $3d^6(^5D)4f$ levels, 1.05 ± 0.02 ea_o^2 for the $3d^6(^5D)5g$ levels, and 1.098 ± 0.008 ea_o^2 for the $3d^6(^5D)6h$ levels. By solving the two equations for the intercepts for the $4f$ and $5g$ levels, an ionization energy of 130 660 ± 5 cm^{-1} is obtained with α = 17.0 ± 0.3. For the $5g$ and $6h$ levels, the ionization energy obtained is 130 655.4 ± 0.4 cm^{-1} with α = 15.0 ± 0.2 a_o^3. The $4f$ levels are not well described by the quadrupole-polarization model as the centers of gravity of the pairs show a large scatter around a straightline as shown in Figure 1. We thus recommend the value 130 655.4 ± 0.4 cm^{-1} obtained from the $5g$ and $6h$ levels.

7. SUMMARY

Table 4 contains 12,887 spectral lines from 13,653 transitions in Fe II, over a factor of three more than the number of previously published lines in Fe II. About 900 of these lines have alternate plausible identifications due to Fe I, Fe III, Ne, Ar, or other Fe II transitions. These lines come from a total list of about 37,000 lines. Roughly 11,500 of the lines in this total list remain unidentified, and about 460 of these lines are present in the FT spectra with an S/N > 50. About half of these strong unidentified lines are in the infrared region and are probably due to highly excited levels in Fe I or Fe II that have yet to be identified. The uncertainties of the strongest lines in Table 4 vary from 0.0001 cm^{-1} in the infrared to 0.001 cm^{-1} in the ultraviolet, and are more than an order of magnitude lower than the best lines in Johansson (1978).

G. Nave thanks Craig J. Sansonetti for many invaluable discussions on wavelength calibration, spectral analysis, and on the best way to approach and present a project of this size. She also thanks Robert L. Kurucz and Alexander E. Kramida for their assistance in finding errors in the tables. James W. Brault, Richard C. M. Learner, Victor Kaufman, and Anne P. Thorne took or assisted with taking many of the spectra used in this paper. Some of these spectra are available in the National Solar Observatory digital Library (Hill & Suarez 2012). This work was partially supported by the National Aeronautics and Space Administration under the inter-agency agreement NNH10AH38I.

REFERENCES

Adam, J., Baschek, B., Johansson, S., Nilsson, A. E., & Brage, T. 1987, ApJ, 312, 337
Aldenius, M. 2009, PhST, 134, 014008
Aldenius, M., Johansson, S. G., & Murphy, M. T. 2006, MNRAS, 370, 444
Batteiger, V., Knünz, S., Herrmann, M., et al. 2009, PhRvA, 80, 022503
Biémont, E., Johansson, S., & Palmeri, P. 1997, PhysS, 55, 559
Brandt, J. C., Heap, S. R., Beaver, E. A., et al. 1999, AJ, 117, 1505
Brault, J. W., & Abrams, M. C. 1989, Fourier Transform Spectroscopy: New Methods and Applications (1989 OSA Technical Digest Series, Vol. 6; Santa Fe, NM: Optical Society of America), 110
Castelli, F., & Kurucz, R. L. 2010, A&A, 520, A57
Castelli, F., Kurucz, R. L., & Hubrig, S. 2009, A&A, 508, 401
Davis, S. P., Abrams, M. C., & Brault, J. W. 2001, Fourier Transform Spectrometry (San Diego, CA: Academic Press)
Dupree, A. K., Lobel, A., Young, P. R., et al. 2005, ApJ, 622, 629
Hamann, F., & Ferland, G. 1999, ARA&A, 37, 487
Hannemann, S., Salumbides, E. J., Witte, S., et al. 2006, PhRvA, 74, 012505
Hill, F., & Suarez, I. 2012, National Solar Observatory Digital Library, http://diglib.nso.edu
Johansson, S. 1978, PhS, 18, 217
Johansson, S. 2009, PhST, 134, 014013
Johansson, S., & Baschek, B. 1988, NIMPB, 31, 222

Johansson, S., Brage, T., Leckrone, D. S., Nave, G., & Wahlgren, G. M. 1995, ApJ, 446, 361
Johansson, S., & Letokhov, V. S. 2004, A&A, 428, 497
Johansson, S., & Litzén, U. 1974, PhS, 10, 121
Kramida, A. E. 2011, CoPhC, 182, 419
Kramida, A. E., & Nave, G. 2006, EPJD, 39, 331
Kurucz, R. 2010, Atomic line data for Fe II: file gf2601.pos created on 23rd July, 2010, http://kurucz.harvard.edu/atoms/2601/gf2601.pos
Learner, R. C. M., & Thorne, A. P. 1988, JOSAB, 5, 2045
Nave, G., Johansson, S., Learner, R. C. M., Thorne, A. P., & Brault, J. W. 1994, ApJS, 94, 221
Nave, G., Johansson, S., & Thorne, A. P. 1997a, JOSAB, 14, 1035
Nave, G., Learner, R. C. M., Murray, J. E., Thorne, A. P., & Brault, J. W. 1992, JPhys2, 2, 913
Nave, G., Learner, R. C. M., Thorne, A. P., & Harris, C. J. 1991, JOSAB, 8, 2028
Nave, G., & Sansonetti, C. J. 2004, JOSAB, 21, 442
Nave, G., & Sansonetti, C. J. 2011, JOSAB, 28, 737
Nave, G., Sansonetti, C. J., & Griesmann, U. 1997b, in Fourier Transform Spectroscopy: New Methods and Applications, (1997 OSA Technical Digest Series, Vol. 3; Santa Fe, NM: Optical Society of America), 38
Peck, E. R., & Reeder, K. 1972, JOSA, 62, 958
Ralchenko, Y., Kramida, A., Reader, J., & NIST ASD Team. 2012, NIST Atomic Spectra Database (version 4.1), http://physics.nist.gov/asd
Rosberg, M., & Johansson, S. 1992, PhS, 45, 590
Saloman, E. B., & Sansonetti, C. J. 2004, JPCRD, 33, 1113
Salumbides, E. J., Hannemann, S., Eikema, K. S. E., & Ubachs, W. 2006, MNRAS, 373, L41
Sansonetti, C. J., Blackwell, M. M., & Saloman, E. B. 2004, NISTJ, 109, 371
Schoenfeld, W. G., Chang, E. S., Geller, M., et al. 1995, A&A, 301, 593
Whaling, W., Anderson, W. H. C., Carle, M. T., Brault, J. W., & Zarem, H. A. 1995, JQSRT, 53, 1
Whaling, W., Anderson, W. H. C., Carle, M. T., Brault, J. W., & Zarem, H. A. 2002, NISTJ, 107, 149